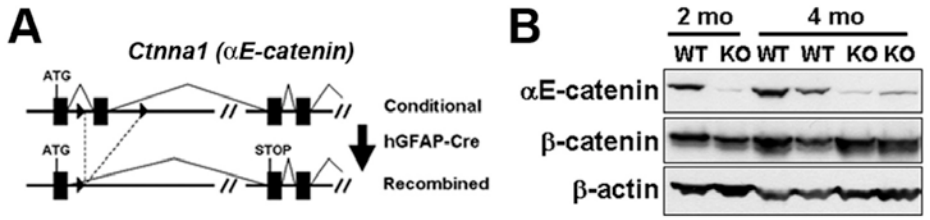

Fig. S1. Generation of *GFAP-Cre/αE-catenin*$^{fl/fl}$ mice. (A) Schematic diagram of conditional deletion of *αE-catenin*. **(B)** Western blot analysis of total skin protein extracts from 2 month-old (2 mo) and 4 month-old (4 mo) wild-type (WT) and *GFAP-Cre/αE-catenin*$^{fl/fl}$ (KO) mice with indicated antibodies.

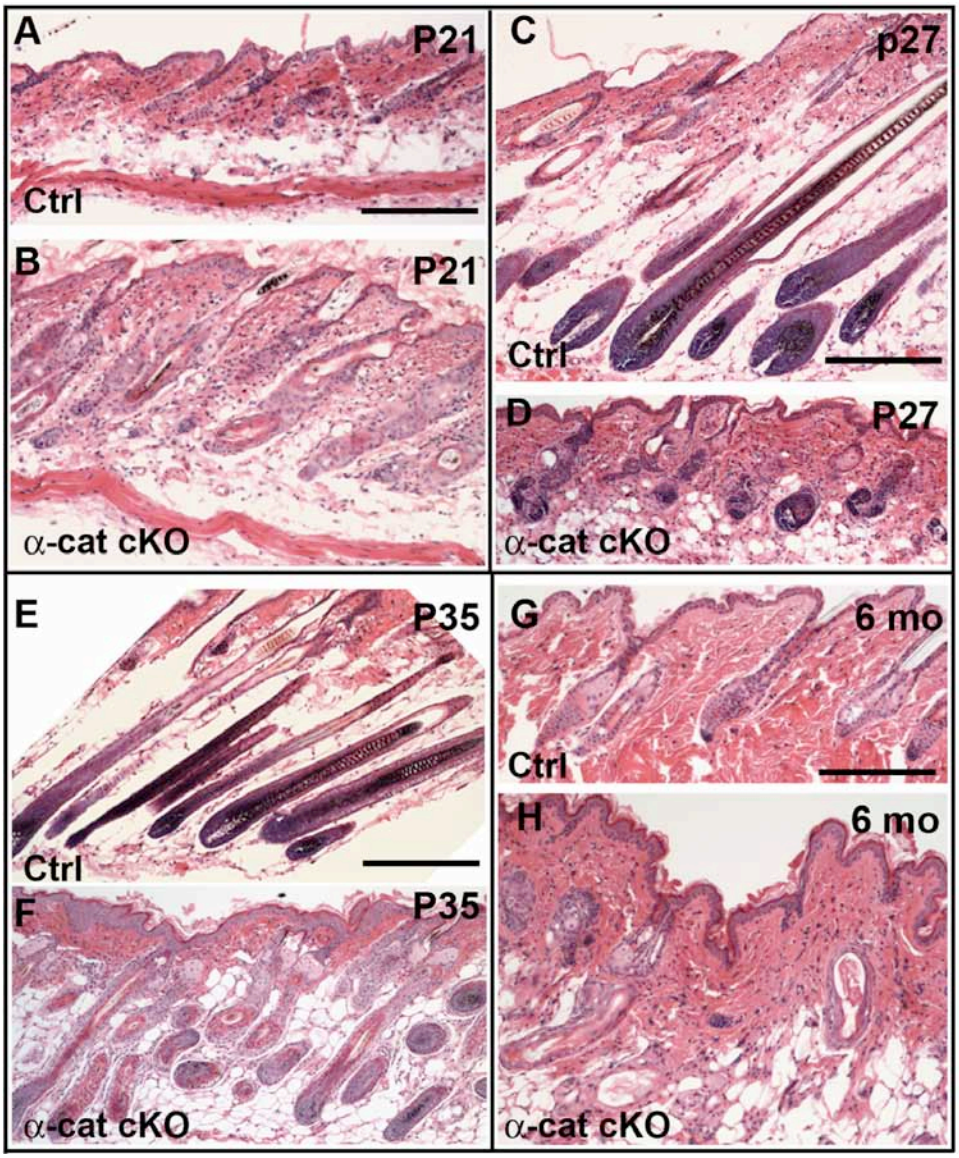

Fig. S2. Skin histology of *GFAP-Cre/αE-catenin*$^{fl/fl}$ mice.
Hematoxylin and eosin staining of skin sections from P21 (A and B), P27 (C and D), P35 (E and F), and 6 month-old (6 mo, G to H) *αE-catenin*$^{fl/fl}$ (Ctrl) and *GFAP-Cre/αE-catenin*$^{fl/fl}$ (α-cat cKO) mice. Scale bars: 168 μm in A, B, G, and H; 252 μm in C and D; and 336 μm in E and F.

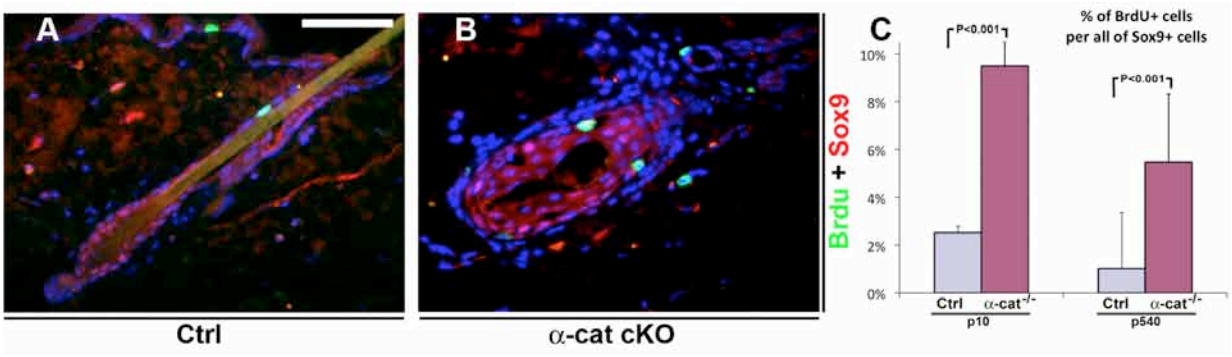

Fig. S3. Increased rates of cell proliferation in *αE-catenin*$^{-/-}$ stem and early progenitor cells. **(A to B)** Immunofluorescent staining of skin sections from P540 *αE-catenin*$^{fl/fl}$ (Ctrl) and *GFAP-Cre*/*αE-catenin*$^{fl/fl}$ (*α*-cat cKO) mice with antibodies against BrdU (green) and Sox9 (stem and early progenitor marker; red). **(C)** Quantification of cells that stained positive for BrdU and Sox9 as a percentage of total Sox9-positive cells within the hair follicles and hair follicle cysts in P10 and P540 *αE-catenin*$^{fl/fl}$ (Ctrl) and *GFAP-Cre*/*αE-catenin*$^{fl/fl}$ (*α*-cat cKO) mice. Bar graph shows mean values ± SD. N=4 for each condition. P values were determined by the Mann-Whitney test. Scale bar, 50 μm.

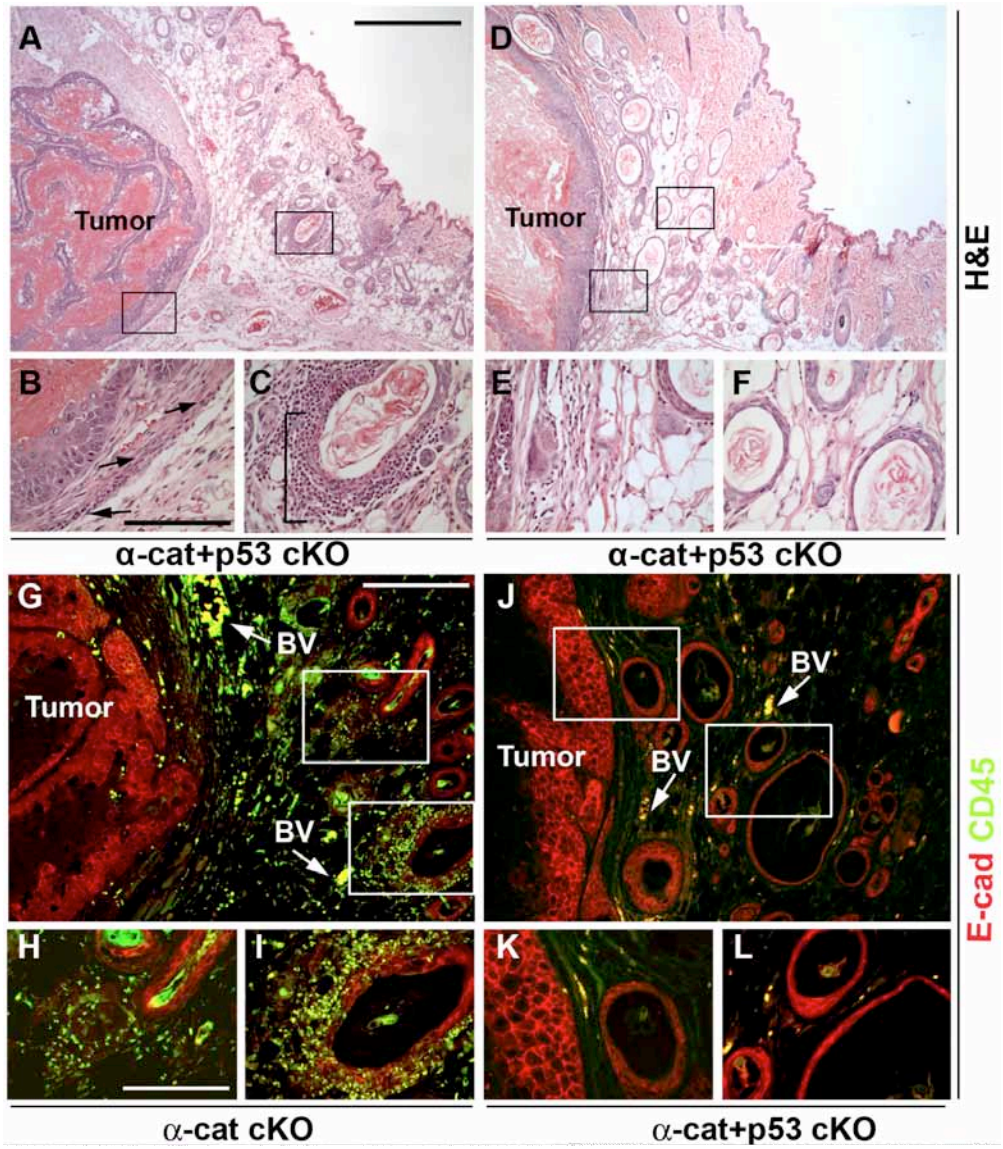

Fig. S4. Inflammatory response in hair follicle cysts and tumors from mice with conditional knockouts of *αE-catenin* or of *αE-catenin* and *p53*.

(A to **F)** Hematoxylin and eosin staining of skin tumors from adult *GFAP-Cre/αE-catenin*$^{fl/fl}$ (*α-cat* cKO) and *GFAP-Cre/αE-catenin*$^{fl/fl}$*/p53*$^{fl/fl}$ (*α-cat+p53* cKO) mice. **(G** to **L)** Immunofluorescence staining of skin tumors and surrounding tissue with anti-E-cadherin (red) and CD45, a marker of leukocyte common antigen, (green) antibodies. Inflammatory cells were present around the cysts and the tumors in the *GFAP-Cre/αE-catenin*$^{fl/fl}$ skin (arrows and brackets in B and C), but were absent in *GFAP-Cre/αE-catenin*$^{fl/fl}$*/p53*$^{fl/fl}$ mice. The areas in the boxes in A, D, G, and J are shown at higher magnification in B, C, E, F, H, I, K, and L. Scale bars: 200 μm in A and D; 55 μm in B, C, E, and F; 90 μm in G and J; and 50 μm in H, I, K, and L.

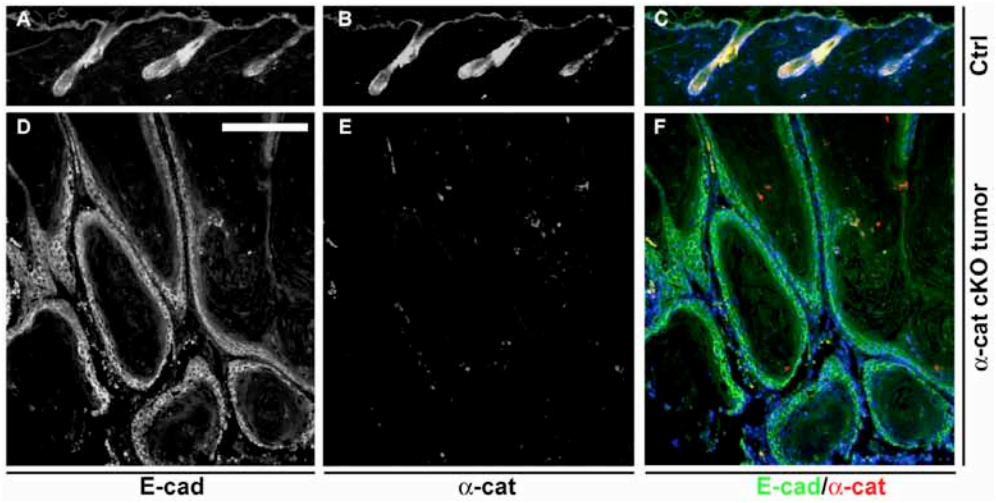

Fig. S5. Tumors in *GFAP-Cre/αE-catenin$^{fl/fl}$* mice are derived from *αE-catenin$^{-/-}$* keratinocytes.

Immunofluorescence staining of sections from *αE-catenin$^{fl/fl}$* skin (Ctrl) and tumors from *GFAP-Cre/αE-catenin$^{fl/fl}$* mice (*α*-cat cKO tumor) with anti-E-cadherin (E-cad) and anti-*α*-catenin (*α*-cat) antibodies. Scale bar, 200 μm for A to F.

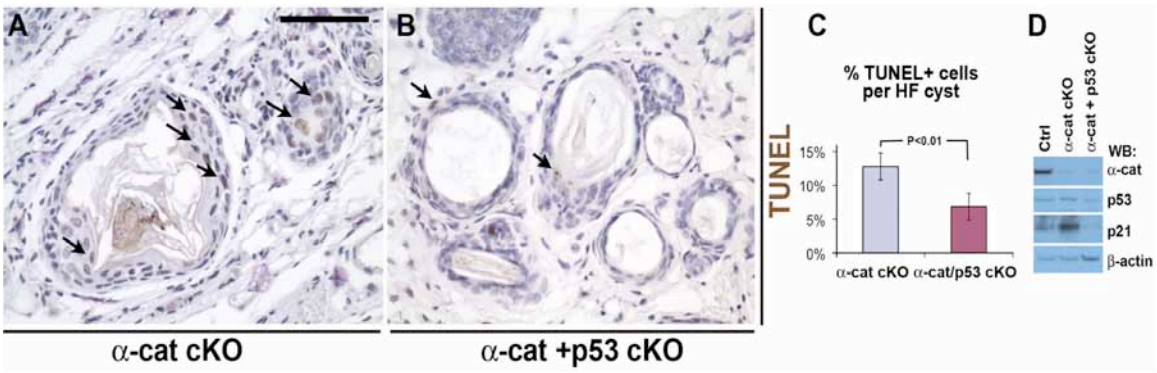

Fig. S6. Apoptosis in hair follicle cysts from mice with conditional knockout of *αE-catenin* or of *αE-catenin* and *p53*.

(A and **B)** TUNEL staining of skin sections from 4 month-old mice. Blue is a nuclear counterstain. Scale bar, 75 μm. **(C)** Quantification of apoptotic cells in the cysts from *GFAP-Cre/αE-catenin*$^{fl/fl}$ (*α-cat* cKO) and *GFAP-Cre/αE-catenin*$^{fl/fl}$/*p53*$^{fl/fl}$ (*α-cat+p53* cKO) mice. Bar graph shows mean values ± SD. Statistical significance was determined by the Mann-Whitney test. **(D)** Western blot (WB) analysis of skin protein extracts from *αE-catenin*$^{fl/fl}$ (Ctrl), *GFAP-Cre/αE-catenin*$^{fl/fl}$ (*α-cat* cKO), and *GFAP-Cre/αE-catenin*$^{fl/fl}$/*p53*$^{fl/fl}$ (*α-cat+p53* cKO) mice with anti-α-catenin, anti-p53, anti-p21, and anti-β-actin antibodies.

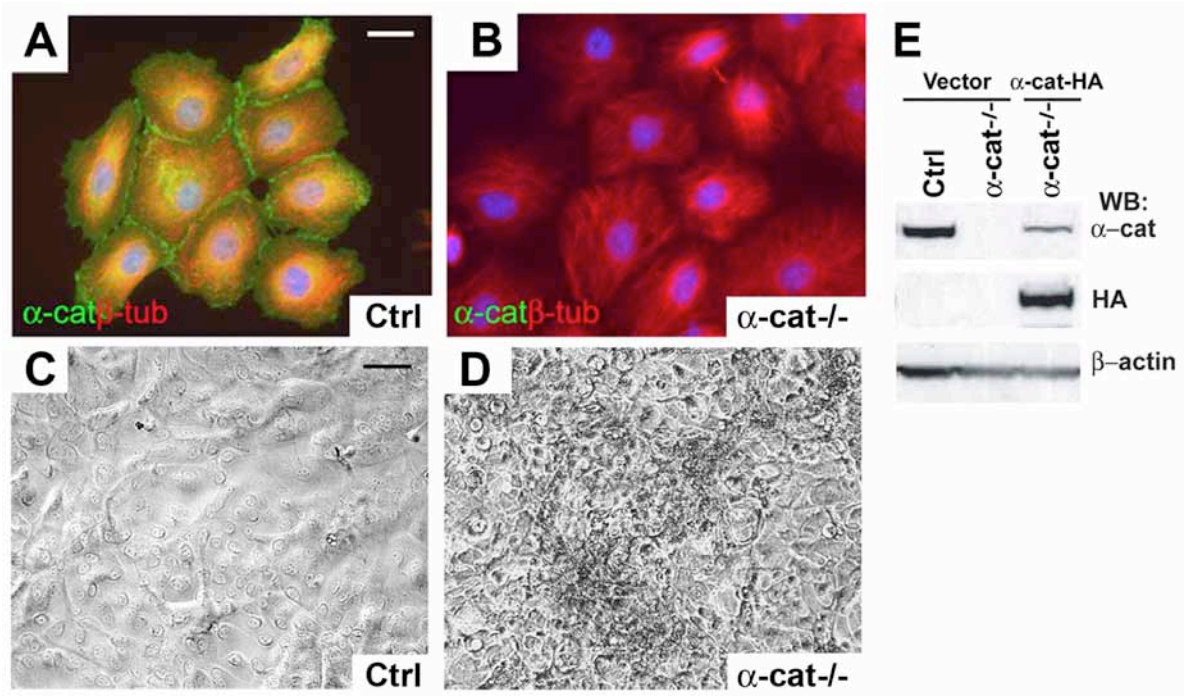

Fig. S7. αE-catenin is necessary for contact-mediated inhibition of cell accumulation.
(**A** to **B)** Immunofluorescent staining of subconfluent *αE-catenin*$^{fl/fl}$ (Ctrl) and *αE-catenin*$^{-/-}$ (*α*-cat$^{-/-}$) keratinocytes with anti-a-catenin (green) and anti-tubulin (red) antibodies. (**C** to **D)** Phase contrast microscopy of confluent *αE-catenin*$^{fl/fl}$ (Ctrl) and *αE-catenin*$^{-/-}$ (*α*-cat$^{-/-}$) keratinocytes. **(E)** Western blot (WB) analysis of proteins from cultured *αE-catenin*$^{fl/fl}$ (Ctrl) and *αE-catenin*$^{-/-}$ (*α*-cat$^{-/-}$) keratinocytes transduced with vector or full-length HA-tagged αE-catenin (*α*-cat-HA) with anti-*α*-catenin, anti-HA and anti-β-actin antibodies. Scale bars: 25 μm in A and B; 75 μm in C and D.

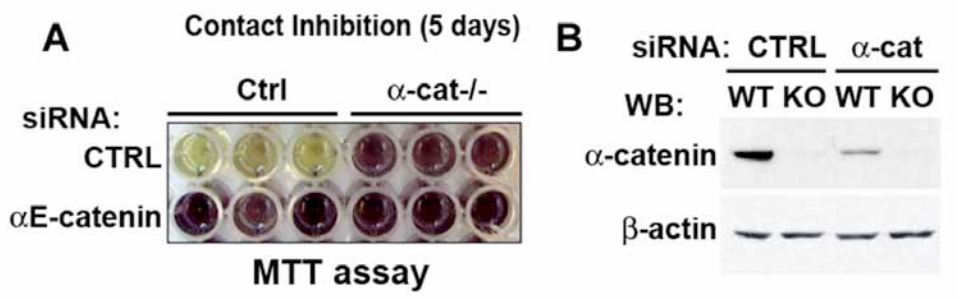

Fig. S8. 96-well plate assay for contact inhibition of cell accumulation.
(A) *αE-catenin*$^{fl/fl}$ or *αE-catenin*$^{-/-}$ keratinocytes were plated at high density in siRNA-Lipofectamine mixture in triplicate and cultured for 5 days. Cell numbers at the end of culture were determined by MTT assay. Under these conditions, *αE-catenin*$^{-/-}$ cells were not contact inhibited and showed increased cell accumulation. This phenotype was replicated in *αE-catenin*$^{fl/fl}$ cells by transfection of siRNAs targeting *αE-catenin*. **(B)** Western blotting demonstrating the efficiency of the knockdown in (A).

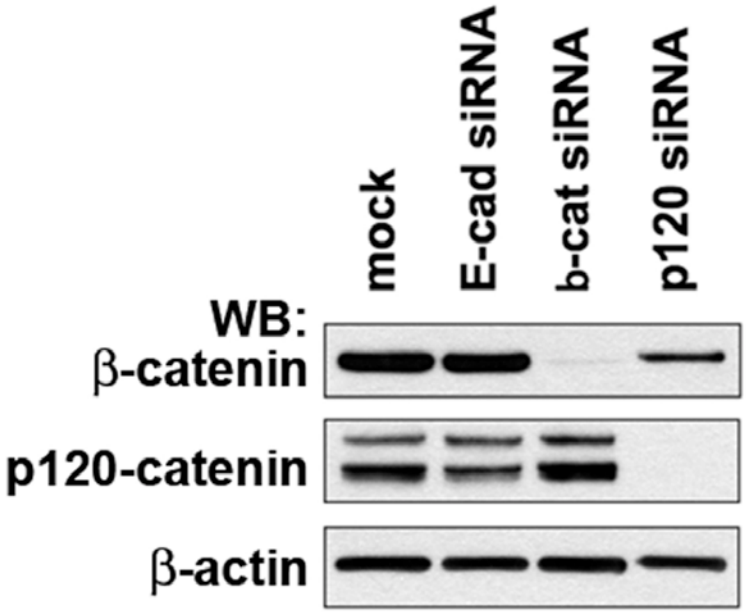

Fig. S9. Efficient knockdown of gene targets after siRNA transfection in 96-well plate contact inhibition assay.

Keratinocytes were plated at high density in siRNA-Lipofectamine mixtures targeting β-catenin or p120-catenin and cultured for 5 days. Total proteins were isolated and analyzed by western blotting with β-catenin and p120-catenin antibodies.

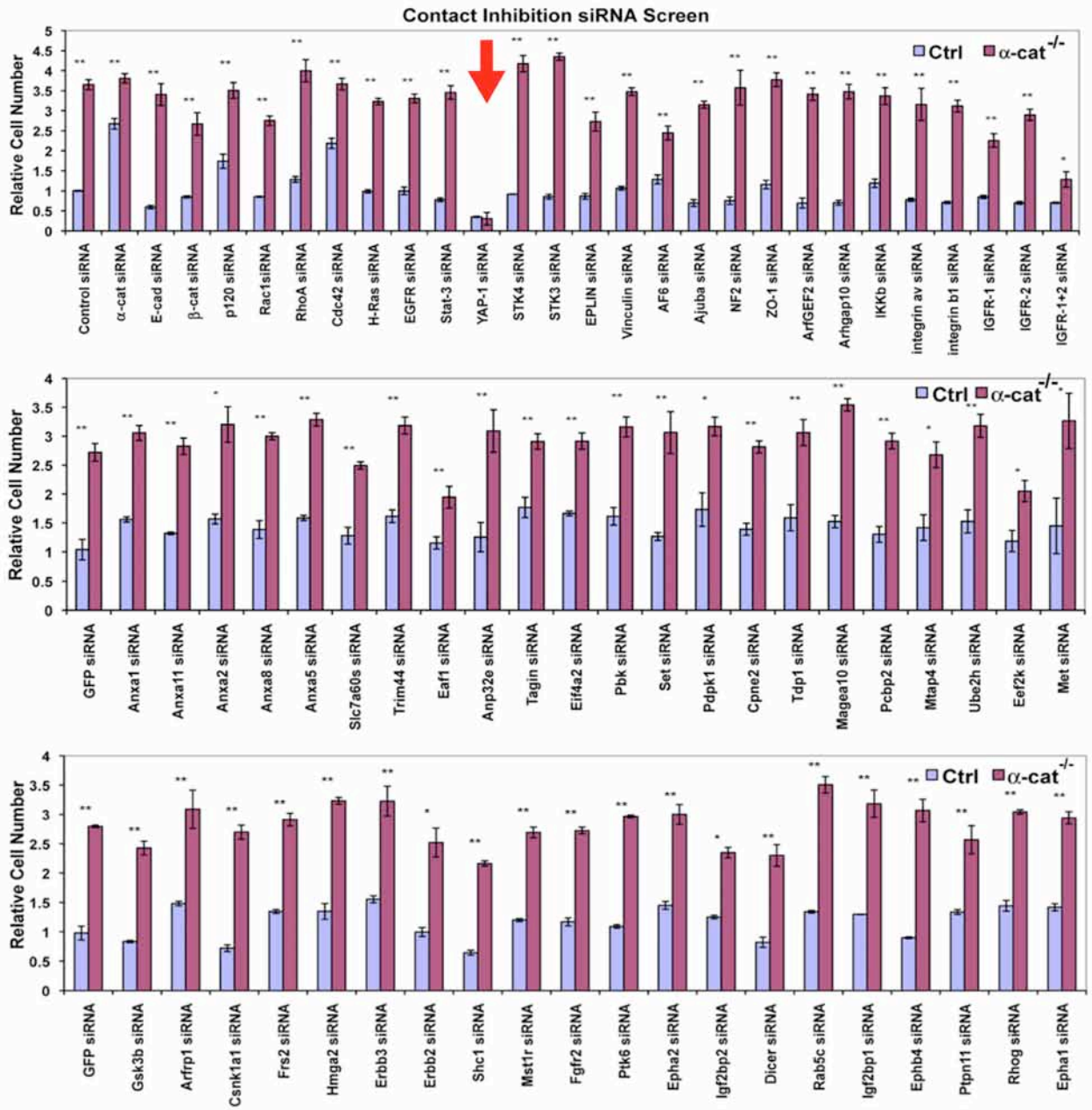

Fig. S10. siRNA screen for genes required for αE-catenin-mediated contact inhibition. *αE-catenin*$^{fl/fl}$ or *αE-catenin*$^{-/-}$ keratinocytes were plated at high density in siRNA-Lipofectamine mixture in triplicate and cultured for 5 days. Cell numbers at the end of culture were determined by MTT assay. A mixture of four independent siRNA oligonucleotides from Qiagen was used to target each indicated gene. Bar graphs show mean values ± SD. N=3. Transfection of siRNA oligos targeting *Yap1* rescues abnormal accumulation of *αE-catenin*$^{-/-}$ keratinocytes.

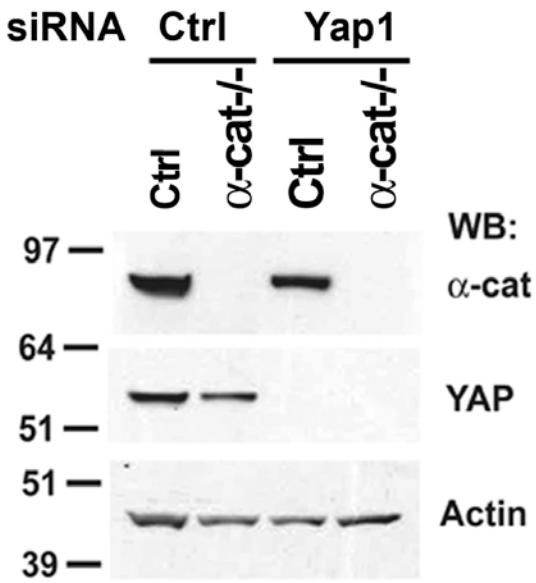

Fig. S11. Efficient knockdown of *Yap1* after transfection of keratinocytes with siRNA oligos.
Keratinocytes were plated at high density in siRNA-Lipofectamine mixture targeting *Yap1* (Dharmacon) and cultured for 5 days. Total proteins were isolated and analyzed by western blotting with anti-α-catenin, anti-Yap1 and anti-β-actin antibodies.

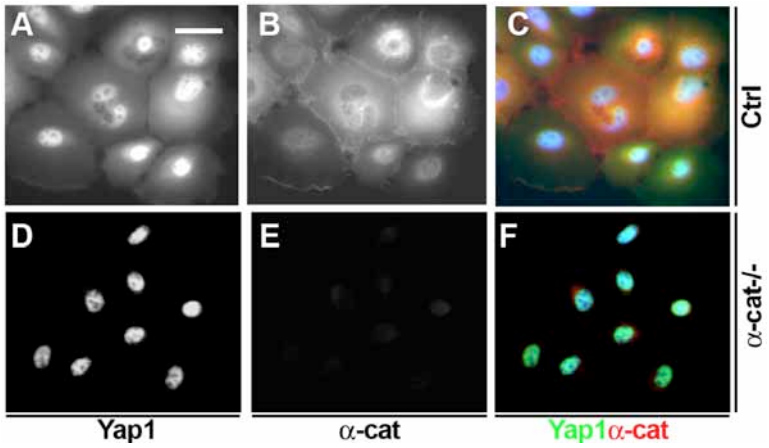

Fig. S12. Nuclear localization of Yap1 in subconfluent *αE-catenin*$^{fl/fl}$ and *αE-catenin*$^{-/-}$ keratinocytes.

Immunofluorescent staining of sub-confluent *αE-catenin*$^{fl/fl}$ (Ctrl) and *αE-catenin*$^{-/-}$ (α-cat$^{-/-}$) keratinocytes with anti-Yap1 and anti-α-catenin (*α-cat*) antibodies. Scale bar, 48 μm.

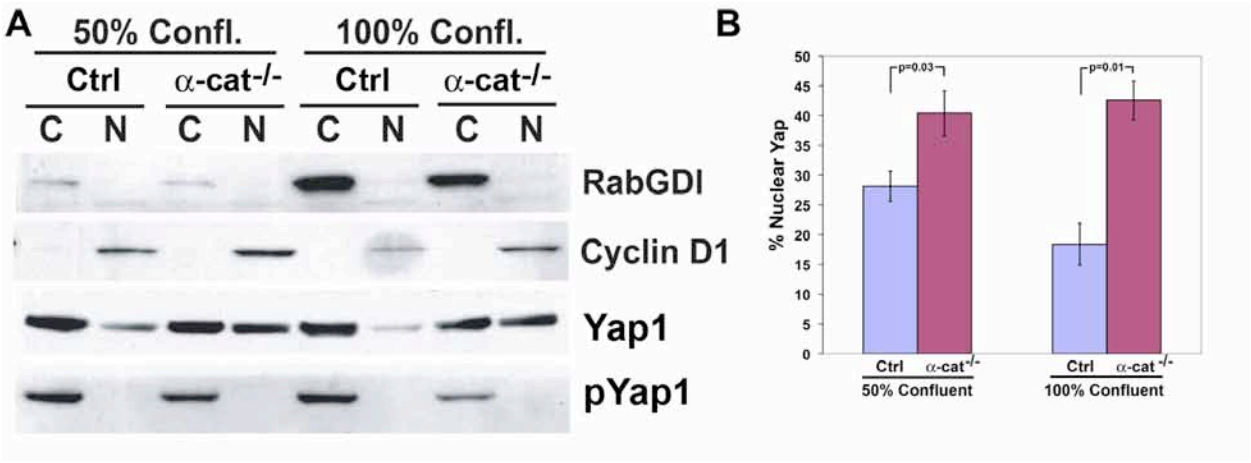

Fig. S13. Increased nuclear localization of Yap1 in confluent *αE-catenin*$^{-/-}$ keratinocytes. **(A)** Proteins extracted from nuclear (N) and cytoplasmic (C) fractions from non-confluent (50%) and confluent (100%) *αE-catenin*$^{fl/fl}$ (Ctrl) and *αE-catenin*$^{-/-}$ (α-cat$^{-/-}$) keratinocytes were analyzed by Western blotting with anti-RabGDI (cytoplasmic protein), anti-cyclin D1 (nuclear protein), anti-Yap1, and anti-phospho-Yap1 (pYap1) antibodies. **(B)** Quantification of the percentage of nuclear compared to total Yap1 in non-confluent (50%) and confluent (100%) *αE-catenin*$^{fl/fl}$ (Ctrl) and *αE-catenin*$^{-/-}$ (α-cat$^{-/-}$) keratinocytes. Bar graph shows mean values ± SD. N=4. P value was determined by the Mann-Whitney test.

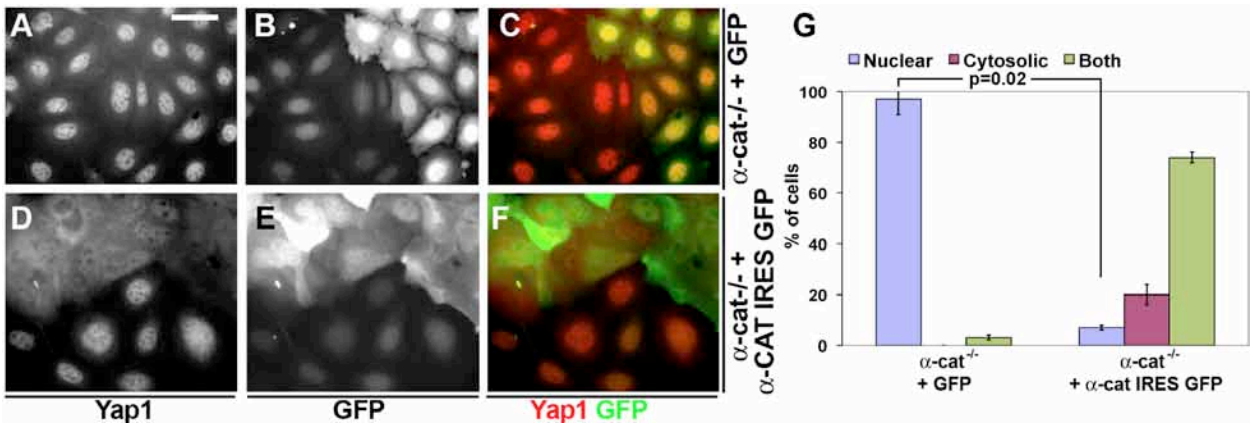

Fig. S14. Rescue of cytoplasmic localization of Yap1 in *αE-catenin*$^{-/-}$ cells transduced with retroviruses expressing full-length αE-catenin.

(A to **F)** Immunofluorescent staining of confluent *αE-catenin*$^{-/-}$ keratinocytes infected with retroviruses expressing control *IRES-GFP* (*α-cat*$^{-/-}$*+GFP) or αE-catenin-IRES-GFP* (*α-cat*$^{-/-}$*+ α-CAT IRES GFP)* with anti-Yap1 antibodies. GFP fluorescence reflected the abundance of transduced protein expression. Yap1 is cytoplasmic in cells with high abundance of retrovirally transduced *α*-catenin (high GFP in E), but not in cells with low abundance of retrovirally transduced *α*-catenin (low GFP in E) or cells expressing high abundance of control empty retrovirus (high GFP in B). Scale bar, 48 μm. **(G)** Quantification of Yap1 localization illustrated in (A) to (F). Bar graph shows mean values ± SD. Number of cells counted was N=90 for GFP; N=87 for α-CAT IRES GFP. P value was determined by Mann-Whitney test.

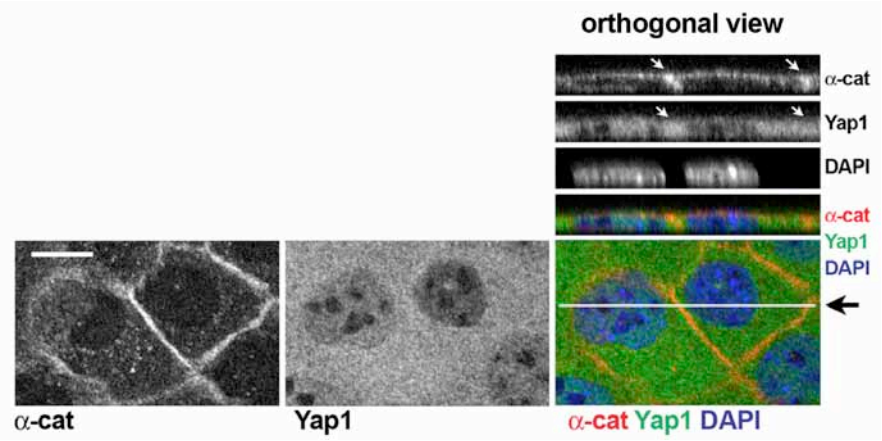

Fig. S15. Partial co-localization between αE-catenin and Yap1 in confluent keratinocytes. High-magnification confocal microscope analysis of *αE-catenin*$^{fl/fl}$ keratinocytes immunostained with anti-Yap1 and anti-α-catenin (α-cat) antibodies. White line indicates the position of orthogonal optical section. DAPI is a nuclear counterstain. Scale bar, 10 μm.

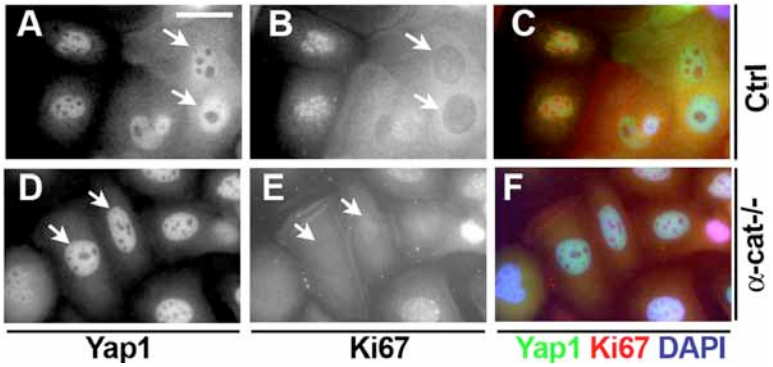

Fig. S16. Yap1 is nuclear in both dividing and non-dividing subconfluent keratinocytes. Immunofluorescent staining of serum-starved subconfluent *αE-catenin*$^{fl/fl}$ (Ctrl) and *αE-catenin*$^{-/-}$ (*α-cat*$^{-/-}$) keratinocytes with anti-Yap1 and anti-Ki67 antibodies. Note nuclear Yap1 in both Ki67-negative and Ki67-positive cells. Scale bar, 21 μm.

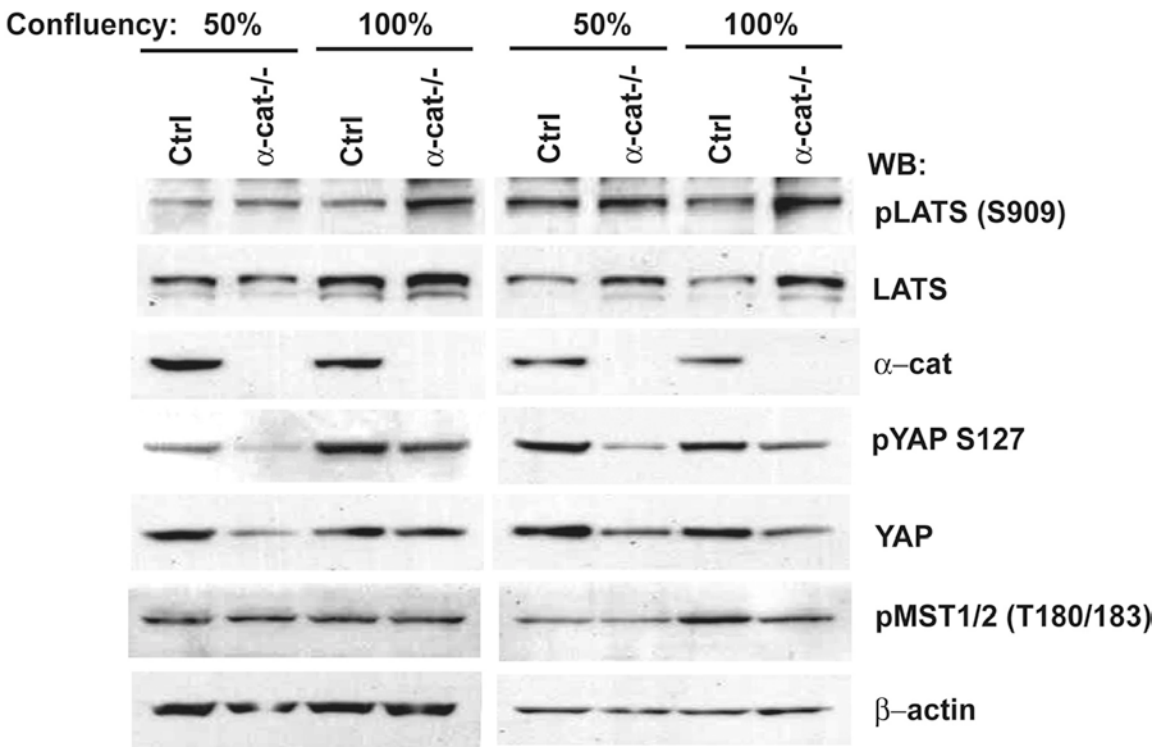

Fig. S17. Western blot analysis of Hippo pathway proteins in cultured keratinocytes. Total protein extracts from non-confluent (50%) and confluent (100%) *αE-catenin*$^{fl/fl}$ (Ctrl) and *αE-catenin*$^{-/-}$ (*α*-cat-/-) keratinocytes with anti-phospho-LATS (pLATS S909), anti-LATS, anti-*α*-catenin, anti-phospho-Yap1 (pYap S127), anti-total Yap1, anto-phospho-MST1/2 (pMST1/2 T180/183), and anti-β-actin antibodies. Representative blots from two independent experiments are shown.

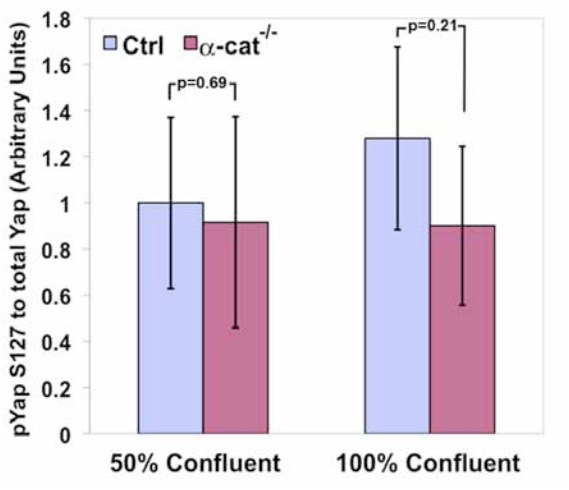

Fig. S18. Quantitation of Yap1 specific phosphorylation on S127.
Total protein lysates from *αE-catenin*$^{fl/fl}$ (Ctrl) and *αE-catenin*$^{-/-}$ (α-cat$^{-/-}$) keratinocytes were analyzed by Western blotting with anti-phospho-Yap1 (pYap S127) and anti-total Yap1 antibodies. The intensities of the bands were measured and the ratios were determined between the phosphorylated and total Yap1 protein levels. Bar graph shows means of normalized ratios ± SD. N=5 for Ctrl and N=5 for (α-cat$^{-/-}$). P values were determined by Mann-Whitney test.

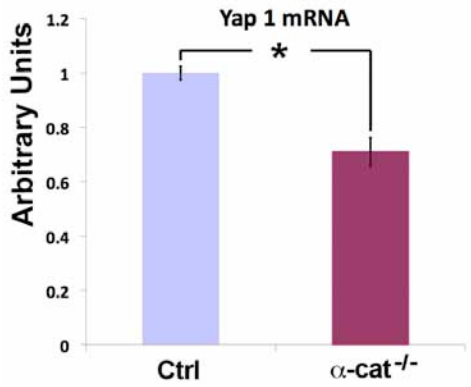

Fig. S19. Decreased abundance of Yap1 mRNA in *αE-catenin*$^{-/-}$ keratinocytes.
Total RNA was extracted from confluent *αE-catenin*$^{fl/fl}$ (Ctrl) and *αE-catenin*$^{-/-}$ (α-cat-/-) keratinocytes and *Yap1* mRNA abundance was determined by qRT-PCR. Bar graph shows mean values ± SD. N=3. P value was determined by Mann-Whitney test. *, P<0.05.

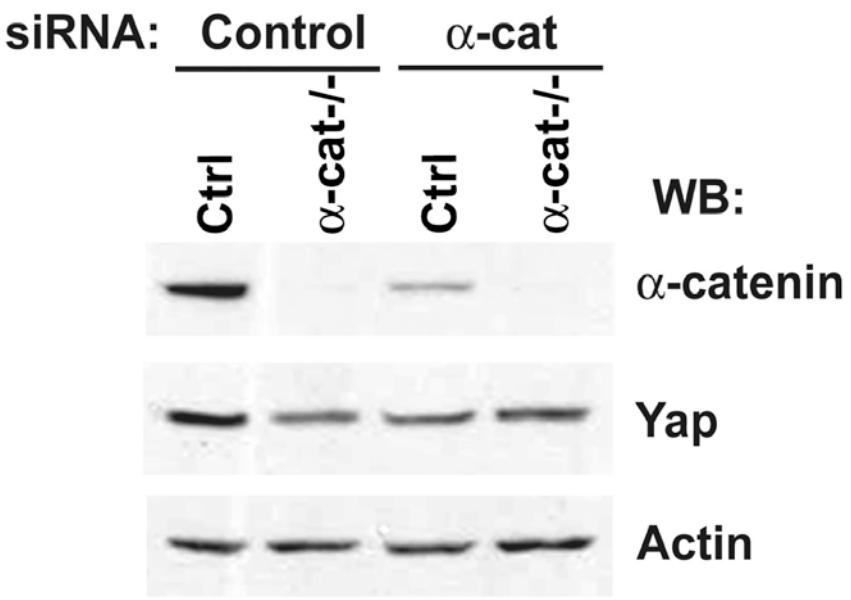

Fig. S20. Acute knockdown of *αE-catenin* reduces total Yap1 protein abundance.
αE-catenin$^{fl/fl}$ (Ctrl) and *αE-catenin*$^{-/-}$ (α-cat$^{-/-}$) keratinocytes were transfected with siRNAs targeting mouse *αE-catenin*. Lysates were collected 48 hours post-transfection and analyzed by Western blotting (WB) for αE-catenin, Yap1, and β-actin. Representative blots from 3 independent experiments are shown.

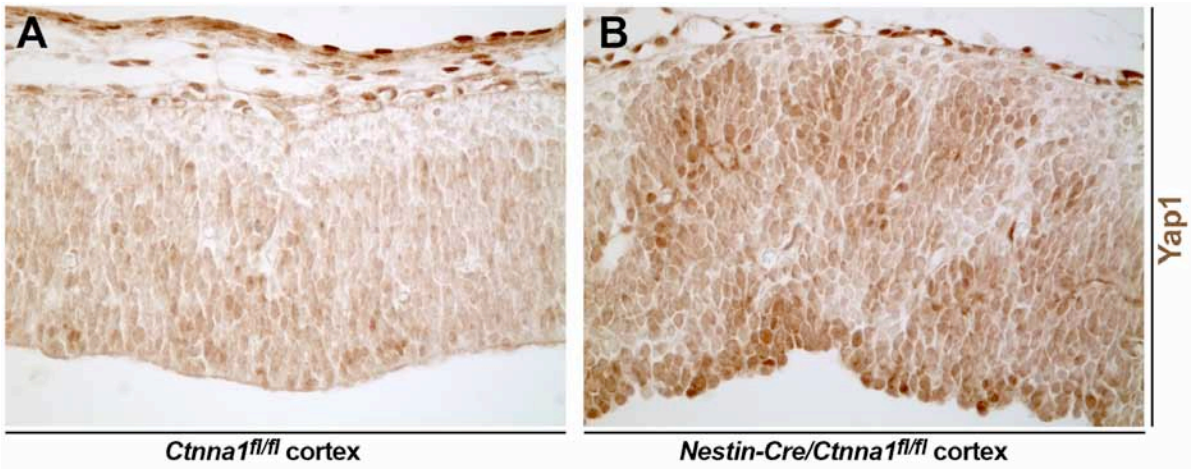

Fig. S21. Nuclear localization of Yap1 in *αE-catenin*$^{-/-}$ cortical neural progenitor cells. Sagittal cortical sections from E12.5 *Nestin-Cre/αE-catenin*$^{fl/+}$ and *Nestin-Cre/αE-catenin*$^{fl/fl}$ embryos (1) were stained with anti-Yap1 antibodies. E12.5 is one day before prominent hyperplasia accompanied by activation of the Hedgehog signaling takes place in the cerebral cortices of *Nestin-Cre/αE-catenin*$^{fl/fl}$ embryos (*1*). Although the mechanisms responsible for activation of the Hedgehog target genes in *αE-catenin*$^{-/-}$ cortical neural progenitor cells remain unknown, it is possible that increased Yap1 signaling is responsible for this phenotype. Yap1 signaling targets are tissue-specific and Yap1 and Hedgehog pathways can amplify each other in the central nervous system (2). Images are representative of N=3 embryos.

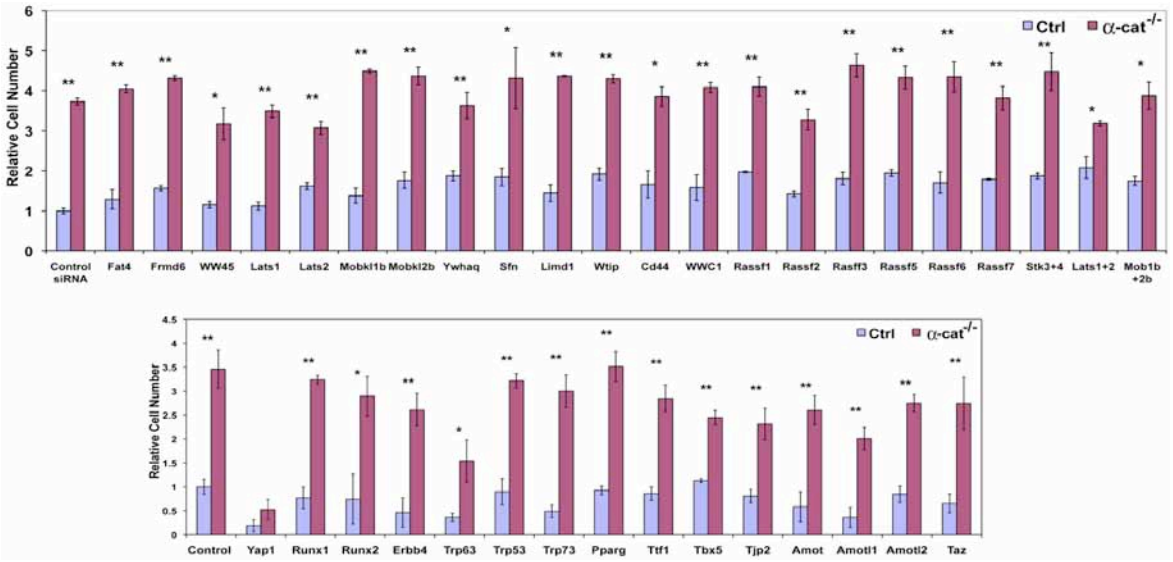

Fig. S22. Hippo pathway siRNA screen on cultured *αE-catenin*$^{fl/fl}$ (Ctrl) and *αE-catenin*$^{-/-}$ (α-cat$^{-/-}$) keratinocytes.

A mixture of 4 independent siRNA oligos (Qiagen) was used to target each indicated gene. The conditions for the assay were similar to Fig. S10. Bar graphs show mean values ± SD. N=3. P values were determined by the Student's t test. **, P <0.01. *, P<0.05.

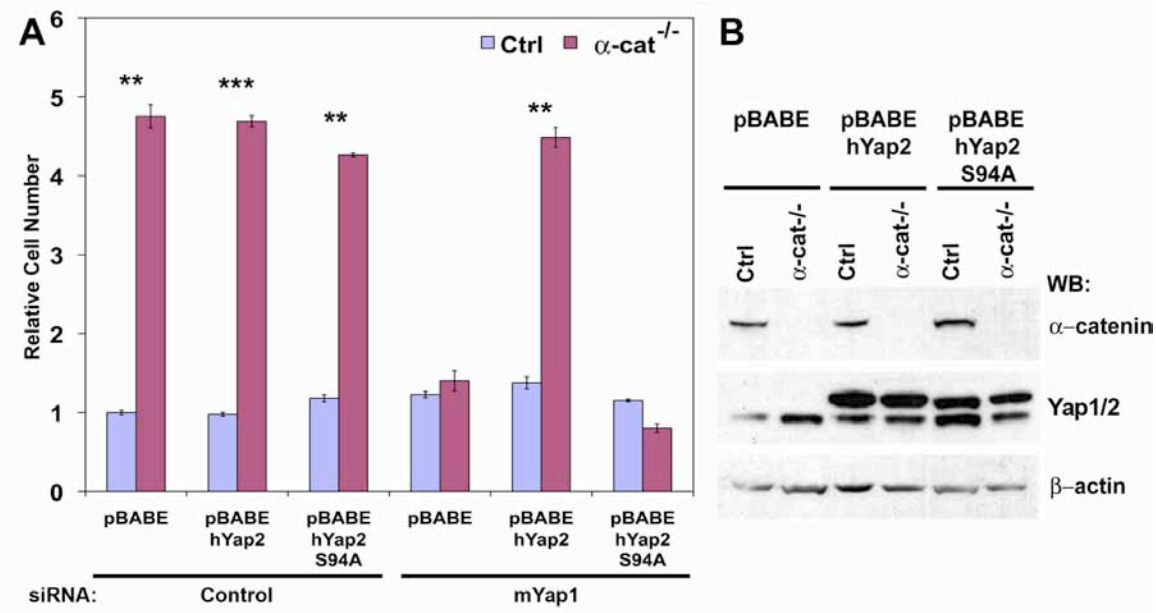

Fig. S23. Wild-type, but not S94A mutant, human Yap2 protein is necessary for increased cell proliferation in *αE-catenin*$^{-/-}$ keratinocytes.

(A) *αE-catenin*$^{fl/fl}$ (Ctrl) and *αE-catenin*$^{-/-}$ (*α*-cat$^{-/-}$) keratinocytes stably expressing wild-type (pBABE hYap2) or mutant (pBABEhYap2S94A) human Yap2 or vector control (pBABE) were transfected with siRNAs targeting mouse Yap1 (mYap1) and analyzed in the contact inhibition assay (Fig. 4E). Increased proliferation in *αE-catenin*$^{-/-}$ keratinocytes is rescued by expression of human Yap2, but of the S94A mutant Yap2 protein. Bar graph shows mean values ± SD. P value was determined by the Student's t test. **, P<0.01. ***, P<0.001. **(B)** Western blot analysis of *αE-catenin*$^{fl/fl}$ (Ctrl) and *αE-catenin*$^{-/-}$ (α-cat$^{-/-}$) keratinocytes stably expressing human Yap2 (pBABE hYap2 and pBABE hYap2S94A) or vector control (pBABE) with anti-αE-catenin, anti-Yap1/2, and anti-β-actin antibodies.

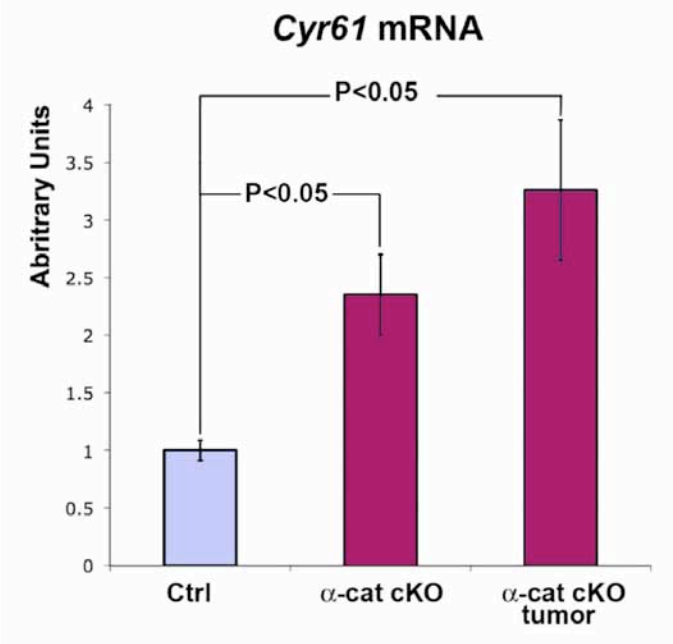

Fig. S24. qRT-PCR analysis of *Cyr61* expression in 4 month old skin and tumors from *αE-catenin*$^{fl/fl}$ (*Ctrl*) and *GFAP-Cre*/*αE-catenin*$^{fl/fl}$ (*α-cat* cKO) mice.
Bar graph shows mean values ± SD. N=3. P value was determined by Mann-Whitney test.

References

1. Lien, W. H., O. Klezovitch, T. E. Fernandez, J. Delrow, and V. Vasioukhin. 2006. alphaE-catenin controls cerebral cortical size by regulating the hedgehog signaling pathway. *Science* 311:1609-1612.
2. Fernandez, L. A., P. A. Northcott, J. Dalton, C. Fraga, D. Ellison, S. Angers, M. D. Taylor, and A. M. Kenney. 2009. YAP1 is amplified and up-regulated in hedgehog-associated medulloblastomas and mediates Sonic hedgehog-driven neural precursor proliferation. *Genes Dev* 23:2729-2741.